# Multicritical End Point of the First-Order Ferromagnetic Transition in Colossal Magnetoresistive Manganites

L. Demkó,[1,2] I. Kézsmárki,[1,2,3] G. Mihály,[1] N. Takeshita,[4] Y. Tomioka,[4] and Y. Tokura[2,3,4]

[1]*Department of Physics, Budapest University of Technology and Economics and Condensed Matter Research Group of the Hungarian Academy of Sciences, 1111 Budapest, Hungary*

[2]*Multiferroics Project, ERATO, Japan Science and Technology Agency (JST), Tsukuba 305-8562, Japan*

[3]*Department of Applied Physics, University of Tokyo, Tokyo 113-8656, Japan*

[4]*Correlated Electron Research Center (CERC), National Institute of Advanced Industrial Science and Technology (AIST), Tsukuba 305-8562, Japan*

(Received 30 November 2007; published 18 July 2008)

We have studied the bandwidth–temperature–magnetic-field phase diagram of $RE_{0.55}Sr_{0.45}MnO_3$ colossal magnetoresistance manganites with ferromagnetic metal (FM) ground state. The bandwidth was controlled both via chemical substitution and hydrostatic pressure with a focus on the vicinity of the critical pressure $p^*$ where the character of the zero-field FM transition changes from first to second order. Below $p^*$ the first-order FM transition extends up to a critical magnetic field. It approaches zero on the larger bandwidth side where the surface of the first-order FM phase boundary is terminated by a multicritical end point. The change in the character of the transition and the decrease of the colossal magnetoresistance effect is attributed to the reduced charge-order and orbital-order fluctuations.

DOI: 10.1103/PhysRevLett.101.037206 PACS numbers: 75.30.Kz, 71.27.+a, 71.30.+h, 75.47.Gk

Perovskite-type manganites exhibit various fundamental phenomena of current interest such as colossal magnetoresistance, photo- and current-induced insulator to metal transitions, first-order ferromagnetic transitions, and the gigantic magnetoelectric effect [1]. One of the most dramatic phase transformations induced by external stimuli is the magnetic-field driven paramagnetic insulator (PI) to ferromagnetic metal (FM) transition. It is observed in a broad temperature range above the Curie temperature and accompanies a huge resistivity change, termed colossal magnetoresistance (CMR). In the context of the CMR effect and the orbital order-disorder transition in manganites, the possibility that the first-order nature of phase transitions in three dimensional systems can be preserved in the presence of disorder has recently attracted much interest [2].

Although the detailed mechanism of the CMR effect is still under debate, some of the basic ingredients have already been clarified. Among them the phase competition between the two robust neighboring states, i.e., the concurrently charge-ordered and orbital-ordered insulator (CO/OO) and the ferromagnetic metal, is thought to be indispensable [1,3]. In the bandwidth-temperature ($w$-$T$) phase diagram of CMR manganites with low quenched disorder, these two phases are separated by a first-order phase boundary which can extend to as high a temperature as $T \approx 200$ K (see Fig. 1). It is terminated by a bicritical point where the CO/OO and FM transition line [$T_{CO}(w)$ and $T_C(w)$, respectively] meet each other. The temperature-induced transition from the high-temperature PI phase to the long-range ordered states on both sides close to the bicritical point is of first order [4–6]. If quenched disorder is introduced to the lattice by alloying rare earth (RE) and alkaline earth (AE) atoms on the $A$ sites with different ionic radii, the phase diagram is strongly modified; the bicritical point is suppressed and a spin-glass state appears between the two ordered phases. On the other hand, the $T_C(w)$ line remains of first order against a large variation of the bandwidth [6].

This situation is shown in Fig. 1 where the typical $w$-$T$ phase diagram of nearly half-doped CMR manganites with large quenched disorder is presented for the series of $RE_{0.55}Sr_{0.45}MnO_3$ where RE = Gd, Eu, Sm, and Nd. The

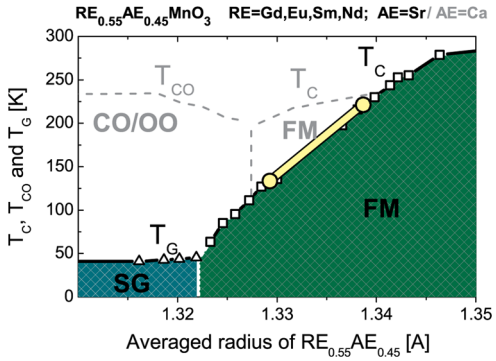


FIG. 1 (color online). Bandwidth-temperature phase diagram of $RE_{0.55}AE_{0.45}MnO_3$ manganites near half-doping with a high level of quenched disorder (reproduced from Tomioka *et al.* [6]). In contrast to the low-disorder case where $T_{CO}$ and $T_C$ meet each other and form the so-called bicritical point as represented by dashed lines, the ordered phases are suppressed and an intermediate spin-glass phase appears below $T_G$. The phase boundaries corresponding to the high- and low-disorder case are shown for the two series, AE = Sr and AE = Ca. In the present Letter the bandwidth of the FM phase was controlled over the highlighted region.

 

variance of the ionic radius on the $A$ site, representing the level of disorder [6,7], is within the range of $\sigma^2 = (0.01 \pm 0.003)$ Å$^2$. The first-order nature of the ferromagnetic phase boundary is robust against the high level of disorder and also extends over a large variation of the bandwidth.

In most ferromagnets, the transition from the high-temperature disordered paramagnetic phase to the ferromagnetic ground state is second order and characterized by a continuous development of the magnetization below $T_C$. Furthermore, the transition exists only in the zero-field limit and becomes a crossover in the presence of an external magnetic field. On the other hand, field-induced metamagnetic transitions between two ordered phases often occur in a first-order manner accompanied with a discontinuous change of the magnetization and a hysteresis. Among a broad variety of such systems [8], the field-induced CO/OO $\mapsto$ FM transition in CMR manganites is a representative example. The first-order nature of the temperature- and field-induced PI $\mapsto$ FM transition generally observed in CMR manganites—either in the vicinity of the bicritical point for low levels of quenched disorder or next to the spin-glass phase when the bicritical point is suppressed—is argued to be the result of enhanced CO/OO fluctuations which are present in a wide temperature range above the FM state [3–6].

In this Letter, we aim to map and characterize the $T_C(w)$ phase boundary of $(Sm_{1-x}Nd_x)_{0.55}Sr_{0.45}MnO_3$ by combining the effects of chemical composition and hydrostatic pressure with a focus on the highlighted region of Fig. 1 where the first-order transition changes to a second-order one. Both methods, the increase of the average ionic radius [6,9–11] and the application of pressure [12,13], increase the one-electron bandwidth and hence the double exchange interaction responsible for the FM phase. We also investigate the effect of magnetic field on the FM transition and determine the $T_C(H)$ phase boundary at each pressure. All the samples investigated here by resistivity and magnetization experiments are single crystals grown by a floating-zone method [11]. For both techniques the application of hydrostatic pressure was carried out using self-clamping pressure cells.

The dramatic increase of $T_C$ in the presence of a magnetic field is characteristic of CMR manganites, especially in the presence of quenched disorder. As shown in Figs. 2(a) and 2(b), the transition is shifted to higher temperatures at an average rate of $\Delta T_C(H)/\Delta H \approx 0.9$ K/kG $= 9$ K/T. Simultaneously, the first-order nature of the transition weakens as clearly reflected by the suppression of the magnetization and resistivity change associated with the transition and also by the reduction of the hysteresis width. For the quantitative analysis we used the latter quantity since it is more reliably obtained from the experimental data. Though no detailed description about the effect of quenched disorder on the thermodynamic and transport properties in the vicinity of a first-order transition

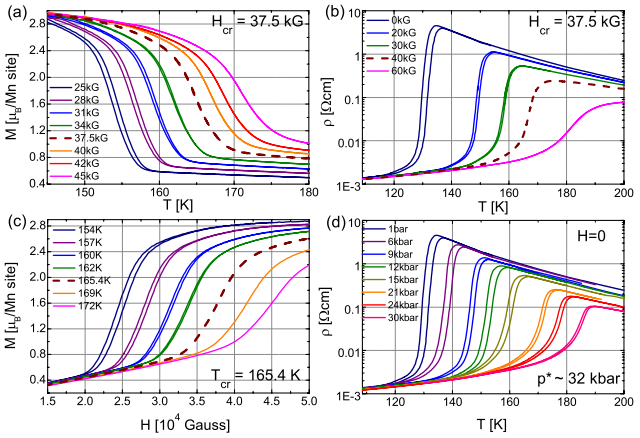


FIG. 2 (color online). Mapping procedure of the pressure–temperature–magnetic-field phase diagram of $Sm_{0.55}Sr_{0.45}MnO_3$ by magnetization and resistivity measurements. Panels (a) and (b) show the temperature dependence of the magnetization and resistivity, respectively, in various magnetic fields. Above the critical field (temperature), $H_{cr}$ ($T_{cr}$) the hysteresis vanishes and the temperature-induced (field-induced) transition becomes a crossover. The corresponding curves are plotted by dashed lines. Panels (c) and (d) display the field dependence of the magnetization at various temperatures and the temperature dependence of the resistivity at selected hydrostatic pressures, respectively.

is available, we attribute the rounding-off in the resistivity and magnetization curves around $T_C$ to the influence of disorder on the nature of the transition [14]. Above a critical magnetic field— $H_{cr} \approx 37.5$ kG in the case of $Sm_{0.55}Sr_{0.45}MnO_3$—the hysteresis completely vanishes and the first-order transition becomes a crossover. Similarly, by performing field sweeps at fixed temperatures above $T_C$, the weakening of the first-order character of the field-driven transition is discerned with increasing temperature [see Fig. 2(c)]. ($T_C$ stands for the zero-field transition temperature, unless field dependence is explicitly indicated.) The hysteresis vanishes above a critical temperature $T_{cr} \approx 165.4$ K for $Sm_{0.55}Sr_{0.45}MnO_3$ at ambient pressure. We call this ($H_{cr}$, $T_{cr}$) point the finite-field critical end point of the first-order FM transition.

The application of pressure extends the FM phase to higher temperatures—$\partial T_C(p)/\partial p \approx 2$ K/kbar as discerned in Fig. 2(d)—while the first-order nature of the transition is again reduced. The critical pressure where the zero-field transition becomes of second order is estimated to be $p^* \approx 32$ kbar for $Sm_{0.55}Sr_{0.45}MnO_3$. A systematic series of experiments, similar to those shown in Fig. 2, were used to map the bandwidth–temperature–magnetic-field phase diagram for the full range of the compounds. In contrast to $T_{cr}(p)$ which is enhanced by pressure in a parallel manner to $T_C(p)$, the critical magnetic field is suppressed according to $H_{cr}(p) \propto (p^* - p)^{1\pm0.05}$ as indicated in Fig. 3. Above the critical pressure $p^*$ the finite-field FM transition no longer exists.

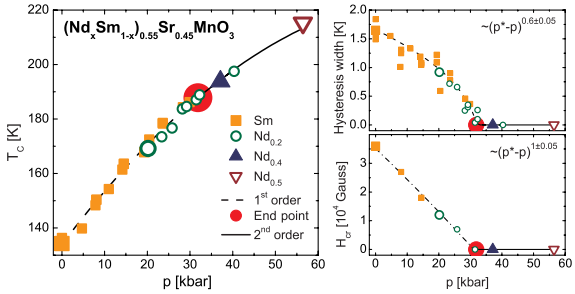


FIG. 3 (color online). Left side: Pressure dependence of the FM transition temperature for $(Sm_{1-x}Nd_x)_{0.55}Sr_{0.45}MnO_3$ ($x = 0, 0.2, 0.4, 0.5$) in zero field. The first- and second-order PI-FM phase boundarise are plotted by dashed and full lines, respectively, while the multicritical end point separating them is labeled by a large full circle. Right upper and lower panel: Hysteresis width observed in the zero-field temperature loops of the resistivity and magnetization curves/critical magnetic field as a function of pressure. The zero-pressure position of the different compounds is indicated by large symbols with $Sm_{0.55}Sr_{0.45}MnO_3$ as the origin of the pressure scales.

The slope of the zero-field phase boundary is unusually small compared with other systems located close to the critical end point of a first-order insulator to metal transition. Representative examples are $(V_{1-x}Cr_x)_2O_3$ [15] and $\kappa - (ET)_2Cu[N(CN)_2]Br$ [16], which undergo a Mott transition by application of pressure from a PI to a PM state. The slope of the first-order transition line—generally related to the jump in the entropy and the volume upon the transition according to the Clausius-Clapeyron equation, $\partial T_C/\partial p = \Delta V/\Delta S$—is $\partial T_C/\partial p \approx 70$ and 300 K/kbar for the former and latter, respectively. Since the volume change accompanying the insulator to metal transition—which is positive in each case as the metallic phase is stabilized under pressure—varies within a factor of 3 for these three compounds [17], the strong distinction in $\partial T_C/\partial p$ is due to the large difference between the change in their entropy. While the spin and orbital sectors are mostly disordered both in the metallic and insulating phases of $(V_{1-x}Cr_x)_2O_3$ and $\kappa - (ET)_2Cu_2(CN)_3$, hence the entropy loss is solely associated with the delocalization of the carriers, in the metallic state of CMR manganites the spin entropy drastically vanishes due to the ferromagnetic ordering. Moreover, there are strong implications that ferro-orbital correlations develop in the FM phase [20,21] further reducing the total entropy.

The evolution of the zero-field $T_C$, the hysteresis width representing the first-order character of the transition, and the critical field $H_{cr}$ as a function of pressure are shown in the respective panels of Fig. 3 in the vicinity of the multicritical end point located at ($p^* \approx 32$ kbar, $T^* \approx 188$ K, $H^* = 0$). The effect of pressure is nearly identical to that of the chemical substitution as the pressure dependence of the transition temperature for the different compounds fits to the same $T_C(p)$ curve when choosing their ambient pressure position adequately [22]. This tendency is valid for the hysteresis width and $H_{cr}(p)$, as well. We also determined the location of the critical point expressed in terms of the relative composition of Nd and Sm and found $x^* \approx 0.33$. The whole pressure–temperature–magnetic-field phase diagram is displayed in the upper panel of Fig. 4 while the lower panel shows the hysteresis width over the corresponding area. The surface of the first-order transition is bordered by two lines: the zero-field phase boundary $T_C(p)$ and the finite-field critical end line $(H_{cr}(p), T_{cr}(p))$. With increasing bandwidth they approach each other and the surface is terminated by the multicritical end point. (Here the term multicritical point means that it terminates a surface of first-order transitions and is not used in the common sense when it separates several thermodynamic phases.) On the larger bandwidth side of the multicritical end point a second-order FM transition line appears where $T_C(p)$ still monotonically increases with pressure.

The first-order nature of the zero-field FM transition is the strongest for $Eu_{0.55}Sr_{0.45}MnO_3$ with the lowest transition temperature $T_C \approx 50$ K and the largest critical field

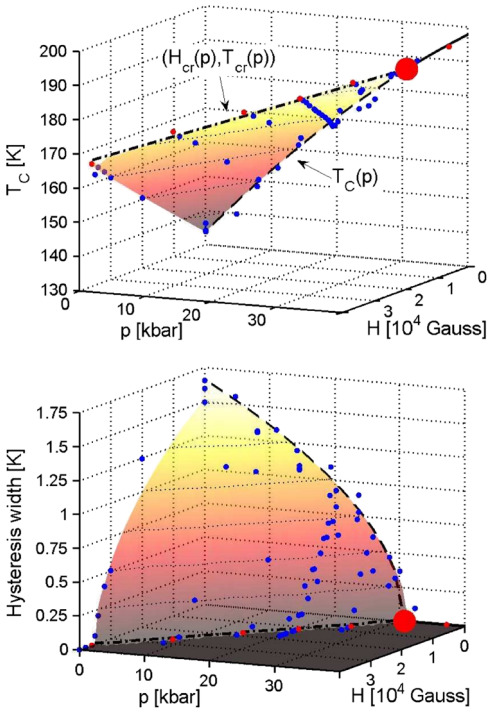


FIG. 4 (color online). Upper panel: PM-FM transition over the pressure–magnetic-field–temperature phase diagram of $(Nd_xSm_{1-x})_{0.55}Sr_{0.45}MnO_3$. Dashed and solid lines represent the zero-field first-order and second-order PM-FM transition, respectively. The dash-dotted line corresponds to the finite-field critical end line terminated by the multicritical end point labeled by the large circle. The surface bordered by the dashed and dash-dotted lines represent the first-order PI-FM phase boundary, as obtained by interpolation of the data points. Lower panel: Width of the temperature hysteresis over the pressure–magnetic-field plane.

$H_{cr} \approx 74$ kG. The hysteresis width is $\sim$14.3 K and the resisitivity jump across the transition is 9 orders of magnitude. Hence, it shows the highest CMR effect among these compounds. Recent x-ray diffuse and Raman scattering measurements [11,23,24] and optical conductivity spectra [25] have revealed that the high-temperature state cannot be regarded as a simple paramagnet with disorder in the spin, charge and orbital sector but it is essentially governed by short-range correlations of the CO/OO phase. The finite correlation length of the CO/OO fluctuations (typically a few lattice constants just above $T_C$) do turn the generally continuous PI $\mapsto$ FM transition to the first-order one.

$Eu_{0.55}Sr_{0.45}MnO_3$ on the verge of the SG-FM phase boundary suffers the most from CO/OO fluctuations. These fluctuations were found to gradually vanish with increasing temperature [11]. Towards larger bandwidth, where $T_C$ is remarkably enhanced, they become less relevant in the vicinity of the transition; thus, the first-order nature weakens. On the other hand, the CMR effect is suppressed parallel with the reduction of the resistivity change upon the transition. Finally, at the multicritical end point the fluctuation-induced first-order transition is replaced by the usual second-order FM transition. The colossal magnetoresistance does still exist beyond this point but it is even less effective due to the rounding-off of the resistivity curves around $T_C$.

In conclusion, by a combination of chemical and hydrostatic pressures, we have studied the bandwidth–temperature–magnetic-field phase diagram of $RE_{0.55}Sr_{0.45}MnO_3$ colossal magnetoresistance manganites with large quenched disorder. The first-order nature of the PI $\mapsto$ FM transition is found to be robust against the $A$-site disorder. We have focused on the larger bandwidth region where the character of the zero-field FM transition changes from first to second order, which occurs at a critical pressure $p^* \approx 32$ kbar. The large entropy change between the two phases, which is the consequence of the interlocking of spin, charge, and orbital degrees of freedom, makes the phase boundary unusually flat as $\partial T_C(p)/\partial p \approx 2$ K/kbar. In an external magnetic field the first-order character of the transition is also suppressed and eventually vanishes at a critical magnetic field $H_{cr}(p)$. Unlike in the zero-field limit controlled by pressure, the FM phase transition no longer exists beyond this point but is replaced by a crossover. This finite-field critical end line approaches the $H = 0$ plane according to $H_{cr}(p) \propto (p^* - p)^{1\pm0.05}$. Consequently, the surface of the first-order FM phase boundary is terminated by a zero-field multicritical end point $(p^*, T^*)$ on the larger bandwidth side. The present results in comparison with microscopic studies on the same systems [11,25] indicate the change in the character of the transition and the weakening of the CMR effect is a consequence of reduced CO/OO fluctuations.

The authors are grateful to N. Nagaosa and S. Onoda for enlightening discussions. This work was supported by Grants-In-Aid for Scientific Research (No. 15104006, No. 16076205, and No. 17340104), MEXT of Japan and the Hungarian Scientific Research Funds OTKA under grants No. F61413 and No. K62441 and Bolyai No. 00256/08/11.

[1] E. Dagotto, *Nanoscale Phase Separation and Colossal Magnetoresistance: The Physics of Manganites and Related Compounds* (Springer-Verlag, New York, 2002); Y. Tokura, Rep. Prog. Phys. **69**, 797 (2006).
[2] K. Pradhan, A. Mukherjee, and P. Majumdar, Phys. Rev. Lett. **99**, 147206 (2007); J. Salafranca and L. Brey, Phys. Rev. B **73**, 214404 (2006); J. S. Zhou and J. B. Goodenough, Phys. Rev. B **68**, 144406 (2003); L. A. Fernandez *et al.*, Phys. Rev. Lett. **100**, 057201 (2008).
[3] S. Murakami and N. Nagaosa, Phys. Rev. Lett. **90**, 197201 (2003).
[4] C. P. Adams *et al.*, Phys. Rev. B **70**, 134414 (2004).
[5] K. H. Kim *et al.*, Phys. Rev. Lett. **88**, 167204 (2002).
[6] Y. Tomioka and Y. Tokura, Phys. Rev. B **70**, 014432 (2004).
[7] J. P. Attfield, Chem. Mater. **10**, 3239 (1998).
[8] K. Penc, N. Shannon, and H. Shiba, Phys. Rev. Lett. **93**, 197203 (2004); H. Ueda *et al.*, Phys. Rev. B **73**, 094415 (2006); S. Seki *et al.*, Phys. Rev. B **75**, 100403 (2007); Y. Narumi *et al.*, J. Phys. Soc. Jpn. **76**, 013706 (2007).
[9] Y. Tomioka and Y. Tokura, Phys. Rev. B **66**, 104416 (2002).
[10] L. Brey and P. B. Littlewood, Phys. Rev. Lett. **95**, 117205 (2005).
[11] Y. Tomioka *et al.*, Phys. Rev. B **68**, 094417 (2003).
[12] Y. Moritomo, A. Asamitsu, and Y. Tokura, Phys. Rev. B **51**, 16 491 (1995).
[13] J. J. Neumeier *et al.*, Phys. Rev. B **52**, R7006 (1995).
[14] Though the shape of the curves and the hysteresis width were insensitive to the speed of the temperature and magnetic-field sweeps ($v_T$ and $v_B$) all the experiments were performed under uniform conditions with $v_T = 0.2$ K/min and $v_B = 0.05$ T/min.
[15] P. Limelette *et al.*, Science **302**, 89 (2003).
[16] M. Souza *et al.*, Phys. Rev. Lett. **99**, 037003 (2007).
[17] The volume change corresponding to a single spin unit, i.e., per V, ET-dimer, or Mn site, is 0.15, 0.36, 0.12 Å$^3$ in $(V_{1-x}Cr_x)_2O_3$ [18], $\kappa - (ET)_2Cu[N(CN)_2]Br$ [16], and $RE_{0.55}Sr_{0.45}MnO_3$ [19], respectively.
[18] A. Jayaraman *et al.*, Phys. Rev. B **2**, 3751 (1970).
[19] C. Marquina *et al.*, J. Magn. Magn. Mater. **226**, 999 (2001).
[20] G. Khaliullin and R. Kilian, Phys. Rev. B **61**, 3494 (2000).
[21] Y. Endoh *et al.*, Phys. Rev. Lett. **94**, 017206 (2005).
[22] H. Y. Hwang *et al.*, Phys. Rev. B **52**, 15046 (1995).
[23] Z. Jirak *et al.*, Phys. Rev. B **61**, 1181 (2000).
[24] R. Mathieu *et al.*, Phys. Rev. Lett. **93**, 227202 (2004).
[25] I. Kézsmárki *et al.*, Phys. Rev. B **77**, 075117 (2008).